Formulation and characterization of wheat bran oil-in-water nanoemulsions

Sara Rebolleda, María Teresa Sanz, José Manuel Benito, Sagrario Beltrán*, Isabel Escudero and María Luisa González San-José

Department of Biotechnology and Food Science. University of Burgos. Plaza Misael Bañuelos s/n. 09001 Burgos. Spain.

Abstract

Wheat bran oil (WBO) has been reported to have an important content of bioactive compounds such as tocopherols, alkylresorcinols, steryl ferulates and other phenolic compounds; however, its poor solubility in water systems restricts its applications in the food industry. This study is focused on the formulation of oil-in-water (O/W) nanoemulsions of WBO in order to improve the bioaccessibility of its active compounds. The influence of oil concentration, surfactant type and concentration, and emulsification method, on the droplet size and stability of the nanoemulsions was investigated. Response surface methodology was used to optimize the conditions for preparing stable nanoemulsions with the minimum droplet size. The optimal nanoemulsion was obtained when 1% of WBO and 7.3% of a surfactant

* Author to whom correspondence should be addressed. Tel.: +34 947 258810. Fax: + 34 947 258831. E-mail: beltran@ubu.es

mixture of Span 80 (37.4%) and Tween 80 (62.6%) were emulsified in water by high intensity ultrasonication for 50 s after pre-emulsification with a high speed blender during 5 min. The optimal nanoemulsion showed good stability along time and antioxidant and tyrosinase inhibitory activities, which make it suitable for use in food applications.

Keywords

Nanoemulsion. Wheat bran oil. Ultrasonication. Response surface methodology. Antioxidant capacity. Tyrosinase inhibition.

Chemical compounds studied in this article

5-(n-nonadecyl)resorcinol (PubChem CID: 161858); α-Linolenic Acid (PubChem CID: 5280934); α-Tocopherol (PubChem CID: 14985); γ-Tocopherol (PubChem CID: 92729); Tween 80 (polyoxyethylene (20) sorbitan monooleate) (PubChem CID: 5281955); Span 80 (sorbitan monooleate) (PubChem CID: 9920342); Tween 20 (polyoxyethylene (20) sorbitan monolaurate) (PubChem CID: 443314)

1. Introduction

There has been growing interest in the utilization of natural antioxidants in the food, beverage and pharmaceutical industries due to the increasing consumer´s demand for substituting synthetic compounds by natural substances. Several vegetal by-products have been proved to be a good source of functional ingredients (Herrero, Cifuentes, & Ibañez, 2006). One of these by-products is wheat bran, which has been successfully extracted using supercritical fluid extraction (SFE) giving rise to extracts that have shown an important content on tocopherols, alkylresorcinols and other phenolic compounds, which provide them with a good antioxidant

activity and tyrosinase inhibitory activities (Rebolleda, Beltrán, Sanz, González-Sanjosé, & Solaesa, 2013; Rebolleda, Beltrán, Sanz, & González-Sanjosé, 2013, 2014).

The enzyme tyrosinase is involved both in the browning of food products and in melanosis in animals. Tyrosinase oxidizes *o*-diphenols to highly reactive *o*-quinones, which can (i) spontaneously polymerize to form compounds of high molecular weight or brown pigments, or (ii) undergo nucleophilic attack by amino acids, proteins, polyphenols, or water to form Michael type addition products, which increase the brown color (Wu, Chang, Chen, Fan, & Ho, 2009). Therefore, the food industry demands tyrosinase inhibitors to prevent the alteration of organoleptic and visual quality of food products (Chen, Song, Qiu, Liu, Huang, & Guo, 2005; Roldán, Sánchez-Moreno, de Ancos, & Cano, 2008; Wu, Chang, Chen, Fan, & Ho, 2009). Preliminary results obtained in our laboratory showed that wheat bran oil (WBO) might have an inhibitory effect on mushroom tyrosinase (Rebolleda, Beltrán, Sanz, González-Sanjosé, & Solaesa, 2013).

Due to its lipophilic character, WBO must be formulated before it can be used for aqueous-based matrix applications. The high stability and low turbidity of nanoemulsions (10-200 nm) make them suitable to incorporate lipophilic active ingredients in aqueous-based food and beverages (McClements, 2011; Yang, Marshall-Breton, Leser, Sher, & McClements, 2012). Furthermore, nanoemulsions have been described as drug delivery systems and as adequate media to overcome instability and to enhance the bioavailability of nutraceuticals (Huang, Yu, & Ru, 2010; Karadag, Yang, Ozcelik, & Huang, 2013; Peshkovsky, Peshkovsky, & Bystryak, 2013; Tadros, Izquierdo, Esquena, & Solans, 2004). For all these reasons, nanoemulsions have an increasing interest in the food, cosmetic and pharmaceutical industries.

Different factors, such as the type of oil and surfactant, and process conditions, influence the physicochemical properties of nanoemulsions (Einhorn-Stoll, Weiss, & Kunzek, 2002;

McClements, 2011). The composition of the dispersed oily phase considerably influences the emulsion quality because of the different densities, viscosities and surface-active ingredients of the different type of oils (Einhorn-Stoll, Weiss, & Kunzek, 2002). Some of the oily phases that have been used for obtaining nanoemulsions are limonene oil (Jafari, He, & Bhandari, 2007; Li & Chiang, 2012), sunflower oil (Leong, Wooster, Kentish, & Ashokkumar, 2009), and medium chain triglycerides (Yang, Marshall-Breton, Leser, Sher, & McClements, 2012; Yuan, Gao, Mao, & Zhao, 2008). These oily phases are in most cases used to dissolve bioactive compounds; however, wheat bran oil obtained by SFE already contains highly bioactive compounds, hence, in this work, WBO will be directly emulsified.

The specific objective of the present work was to optimize some process variables, such as oil concentration, surfactant type and concentration, and emulsification method, to obtain stable wheat bran oil-in-water (O/W) nanoemulsions with the minimum possible droplet size. Response surface methodology (RSM) was applied to detect the optimal conditions. Additionally, emulsion stability along time, antioxidant activity and inhibitory effect of the optimal nanoemulsion on mushroom tyrosinase, were evaluated.

2. Experimental section

2.1. Materials

Oil phase: wheat bran oil was obtained by SFE in a semi-pilot plant at 25.0 ± 0.1 MPa, 40 ± 2 ºC and 8 ± 1 kg CO_2/h. Co-extracted water was separated from WBO by centrifugation at 12857*g* during 30 minutes. This WBO was fairly rich in some bioactive compounds such as alkylresorcinols (47 mg/g), mainly 5-(n-nonadecyl)resorcinol (14.3 mg/g) and 5-(n-uneicosyl)resorcinol (22.4 mg/g), α-linolenic acid (37 mg/g), steryl ferulates (18 mg/g), tocopherols (7 mg/g) and phenolic compounds (25 ppm). A wider characterization of the

87 WBO used in this work, including fatty acid profile, has been reported elsewhere (Rebolleda,
88 Beltrán, Sanz, González-Sanjosé, & Solaesa, 2013; Rebolleda, Beltrán, Sanz, & González-
89 SanJosé, 2014) WBO was stored at -20 ºC until the emulsification experiments were
90 performed.

91 *Surfactants:* Several food grade surfactants have been selected in order to achieve the
92 stabilization of O/W nanoemulsions. Table 1 compiles the different surfactants and mixtures
93 of surfactants used, together with their HLB (hydrophilic-lipophilic balance) number. Tween
94 80 (polyoxyethylene (20) sorbitan monooleate) and Span 80 (sorbitan monooleate) were
95 supplied by Sigma-Aldrich Co. (St. Louis, MO, USA), Tween 20 (polyoxyethylene (20)
96 sorbitan monolaurate) by Panreac (Barcelona, Spain) and DATEM (diacetyl tartaric acid ester
97 of mono- and diglycerides) by EPSA (Valencia, Spain).

98 *Water phase:* milli-Q water (Millipore, Billerica, MA, USA) was used for preparing all the
99 emulsions.

100 *Reactants used for determining antioxidant and tyrosinase inhibition activities:* ABTS (2,2′-
101 azino-bis (3-ethylbenzothiazoline-6-sulfonic acid) diammonium salt), Trolox (6-hydroxy-
102 2,5,7,8-tetramethylchromane-2-carboxylic acid), DPPH (2,2-diphenyl-1-picryhydrazyl) and
103 TPTZ (2,4,6-Tri(2-pyridyl)-*s*-triazine), L-DOPA (3,4-dihydroxy-L-phenylalanine) and
104 mushroom tyrosinase are from Sigma–Aldrich Co. (St. Louis, MO, USA). $K_2O_8S_2$, $FeCl_3$ and
105 $FeSO_4$ are from Panreac (Barcelona, Spain).

106 2.2. Equipment and procedure

107 A vortex (VWR, Radnor, PA, USA), a high speed blender (Miccra D9 equipped with a DS-
108 5/K-1 rotor-stator, ART Labortechnik, Mülhein, Germany), an ultrasonic bath (Selecta
109 Ultrasounds H, Barcelona, Spain) and a high intensity ultrasonic processor (Sonics VCX 500,

Newtown, CT, USA) were the apparatuses used for preparing the emulsions. The high intensity ultrasonic processor (500 W, 20 kHz) was used with a titanium alloy microtip probe of 3 mm diameter, at 20% amplitude and in pulses of 5 seconds (5 s ultrasound and 5 s pause) to avoid heating of the sample.

To prepare an emulsion, WBO and surfactant were mixed before water milli-Q was added. Quantities of each emulsion ingredient were measured using an analytical balance (Sartorius, accurate ± 0.0001). The characterization of the emulsions was performed an hour after emulsification to avoid any creaming or coalescence effect.

2.3. Nanoemulsions characterization

Droplet size distribution, mean droplet diameter and polydispersity index (PDI) of samples were measured by dynamic light scattering (DLS) using a Zetasizer Nano ZS apparatus (Malvern Instruments Ltd., UK). The apparatus is equipped with a He-Ne laser emitting at 633 nm and with a 4.0 mW power source. The instrument uses a backscattering configuration where detection is done at a scattering angle of 173º. Samples were first diluted 1:100 to avoid multiple scattering effects and then 2 mL samples were poured into DTS0012 square disposable polystyrene cuvettes. Measurements were performed at 20 ºC. The hydrodynamic diameter was calculated using the Stokes-Einstein equation with the assumption that the particles were monodisperse spheres.

Zeta potential was measured using the aforementioned Zetasizer Nano ZS apparatus. The measurement was conducted for each diluted sample at 20 ºC using DTS1061 disposable folded capillary cells. The Zeta potential, ζ, was calculated from oil droplet electrophoretic mobility measurements in an applied electric field using the Smoluchowski approximation.

The refractive index of the dispersed phase, WBO, was experimentally determined (Milton Roy abbe-type refractometer, Ivyland, PA, USA) resulting to be 1.476 at 25 ºC.

The pH of the nanoemulsions was measured by means of a glass pH electrode (Crison, Barcelona, Spain).

Turbidity analysis of the formulated emulsions was carried out by measuring the absorbance of undiluted samples at 600 nm (Hitachi U-2000 spectrophotometer, Tokyo, Japan) (Ghosh, Mukherjee, & Chandrasekaran, 2013).

2.4. Evaluation of nanoemulsions stability

Stability of wheat bran oil in water nanoemulsions was measured in terms of their droplet growth ratio. Since emulsions tend to aggregate during storage, the droplet size of the emulsions obtained in this work was measured at 15 and 30 days at the bottom of the cell containing them. Two different storage conditions were evaluated: 4 ºC and darkness and 20 ºC and lightness.

Additionally, optical characterization of creaming stability was made for the optimal nanoemulsion using a Turbiscan Lab Expert equipment (Formulaction Co., L'Union, France) by static multiple light scattering (MLS), sending a light beam from an electroluminescent diode (λ = 880 nm) through a cylindrical glass cell containing the sample. The nanoemulsion sample without dilution was placed in a cylindrical glass cell and two synchronous optical sensors received the light transmitted through the sample (180º from the incident light) and the light backscattered by the droplets in the sample (45º from the incident light). The optical reading head scans the height of the sample in the cell (about 40 mm), by acquiring transmission and backscattering data every 40 μm. Transmitted and backscattered light were

154 monitored as a function of time and cell height for 60 days at 25 ºC (Allende, Cambiella,
155 Benito, Pazos, & Coca, 2008).

156 2.5. Evaluation of nanoemulsions antioxidant activity

157 Antioxidant properties of optimal WBO nanoemulsions were evaluated by using the ABTS,
158 DPPH and FRAP methods (Rebolleda, Beltrán, Sanz, González-Sanjosé, & Solaesa, 2013;
159 Rebolleda, Beltrán, Sanz, & González-SanJosé, 2014).

160 *ABTS:* The radical was produced by reaction of 7 mM solution of ABTS in water with
161 2.45 mM $K_2O_8S_2$ (1:1) during 16 h at room temperature and darkness (Rivero-Pérez, Muñiz,
162 & González-Sanjosé, 2007). 20 µL of nanoemulsion were mixed with 980 µL of radical
163 $ABTS^{\bullet+}$ previously diluted until obtaining 0.8 absorbance units at 734 nm (Hitachi U-2000
164 spectrophotometer). The discoloration produced after 20 min reaction is directly correlated
165 with the antioxidant capacity of the products. Trolox was used as standard compound.

166 *DPPH:* 20 µL of nanoemulsion were mixed with 980 µL of $DPPH^{\bullet}$ solution (50.7 µM). The
167 absorbance at 517 nm was measured after 60 min reaction at ambient temperature and
168 darkness. The discoloration produced is directly correlated with the antioxidant capacity of
169 the products. Trolox was used as standard compound.

170 *FRAP:* The FRAP reagent was prepared by mixing 25 mL of 0.3 M sodium acetate buffer
171 solution at pH 3.6, 2.5 mL of a 10 mM solution of TPTZ dissolved in HCl 40 mM, 2.5 mL of
172 $FeCl_3$ (20 mM), and 3 mL of milli-Q water. 30 µL of nanoemulsions were mixed with 970 µL
173 of FRAP reagent. The reaction was carried out at 37 ºC during 30 minutes and the absorbance
174 was measured at 593 nm (Hitachi U-2000 spectrophotometer). $FeSO_4$ was used for
175 calibration. The reductive power of the nanoemulsions was expressed as µmol Fe (II).

2.6. Determination of tyrosinase inhibition activity

The effect of the nanoemulsions on the *o*-diphenolase activity was monitored by the formation of dopachrome at 490 nm. The reaction medium (0.2 mL) contained 0.5 mM L-DOPA prepared in a 100 mM phosphate buffer of pH 7; 0.1 mg/mL of mushroom tyrosinase also prepared in a 100 mM phosphate buffer of pH 7; and different concentrations (0.5 to 2.5 %, v/v) of the nanoemulsion. The absorbance at 490 nm was continuously monitored over a time period of 5 minutes (Labsystems Multiskan MS microplate reader). The initial reaction rate in the presence or absence of the nanoemulsions was calculated from the slope of the reaction curve and the inhibition (%) of the nanoemulsions was calculated as follows:

$$\% \text{ Inhibition} = [1- (Vi-V/Vo-V)] \times 100 \quad (1)$$

where Vi and Vo are the initial reaction rates in the presence or absence of nanoemulsion respectively and V is the initial reaction rate in the absence of mushroom tyrosinase.

The concentration of nanoemulsion that causes 50% enzyme inhibition (IC50) was estimated by plotting the experimental data of inhibition (%) vs. nanoemulsion concentration.

2.7. Experimental design

The effect of two of the factors under study, surfactant type and emulsification procedure, on emulsion formation was firstly studied. Then, response surface methodology (RSM) and central composite design (CCD) were used to study the effect of oil and emulsifier concentration and emulsification time, on the droplet size of the nanoemulsions.

The experiments performed to select the surfactant are presented in Table 1. Emulsions of wheat bran oil (1% w/w) with different emulsifiers (1% w/w) were obtained working with the high speed blender at 29000 rpm during 5 minutes. Each experiment was replicated twice.

198 The emulsification method was selected by preparing different emulsions of wheat bran oil
199 (1% w/w) using the surfactant (1% w/w) selected in the previous assays. The emulsification
200 procedures used in each experiment are shown in Table 2. Each experiment was replicated
201 twice.

202 After selecting the surfactant type and emulsification method, response surface methodology
203 (RSM) was used to study the effect of oil concentration (X_1: 1-10% w/w), emulsifier
204 concentration (X_2: 1-10% w/w) and ultrasonication time (X_3: 50-300 s) on the droplet size of
205 the nanoemulsions (Y). A central composite design (CCD) with three levels of each
206 independent variable (Table 3) was used. The model generated 17 experimental settings with
207 three replicates in the central point. The design was carried out by duplicate.

208 A low degree polynomial equation (second-order one) was used to express predicted
209 responses (Y) as a function of the independent variables under study (X_1, X_2 and X_3). The
210 model equation is as follows:

211 $$Y = a_0 + a_1 X_1 + a_2 X_2 + a_3 X_3 + a_{11} X_1^2 + a_{22} X_2^2 + a_{33} X_3^2 + a_{12} X_1 X_2 +$$

212 $$a_{13} X_1 X_3 + a_{23} X_2 X_3 \qquad (2)$$

213 where Y represents the response variable (droplet size in this case), α_o is a constant, and α_i, α_{ii},
214 α_{ij} are the linear, quadratic and interactive coefficients, respectively. The significance of each
215 estimated regression coefficient was assessed through values of the statistic parameters, F and
216 p (*probability*). The experimental design and data analysis were performed using
217 STATGRAPHICS Centurion XVI (Statpoint Technologies, Inc., Warrenton, VA, USA).

2.8. Statistical analysis

Experimental data were analyzed by simple statistic parameters in order to detect anomalous data and to express results through the average values and the corresponding standard deviation.

Analysis of variance (ANOVA) and LSD test were applied to detect the effect factor and the statistically significant differences among values, respectively.

Data analysis was performed using STATGRAPHICS Centurion XVI (Statpoint Technologies, Inc., Warrenton, VA, USA).

3. Results and discussion

3.1. Influence of surfactant type on nanoemulsion droplet size.

The type of surfactant or mixture of surfactants used for formulating the different emulsions prepared for this study is presented in Table 1 together with their HLB number. Table 1 also shows the droplet size and PDI of the emulsions formulated with the different surfactant systems.

ANOVA analysis showed surfactant factor effect and all the analytical values were statistically different among them. The minimum droplet size (84.6 ± 1.3 nm) and the narrowest particle size distribution (PDI = 0.257 ± 0.009) were obtained when the mixture of Span 80 (37.4%) and Tween 80 (62.6%), with a HLB value of 11, was used. This agrees with empirical observations that suggest that minimum droplet size and maximum emulsion stability is obtained for O/W emulsions when using surfactants with a HLB number within the range 10-12 (McClements, 2005).

According to the results obtained in this section, the experiments presented in the next sections were carried out using the above mentioned surfactant mixture.

3.2. Influence of the emulsification method on nanoemulsion droplet size

The energy needed for the emulsification process can be provided by mechanical agitation, (e.g.: stirring, high shear mixing), high-pressure homogenization or high power ultrasound (Huang, Yu, & Ru, 2010; Peshkovsky, Peshkovsky, & Bystryak, 2013). Although high-pressure homogenization is widely used, ultrasonic methods have several advantages, such as lower-cost equipment, smaller footprint and easier cleaning and servicing (Peshkovsky, Peshkovsky, & Bystryak, 2013).

Some assays were carried out in order to choose the emulsification method that provided an emulsion with a small droplet size (Table 2). ANOVA analysis showed emulsification procedure factor effect. Although the methods using high speed blender happened to bring the smallest droplet size, samples exhibited visual creaming instability after a few hours of storage. In contrast, nanoemulsions obtained with the high intensity ultrasonic processor showed a slightly larger droplet size but visual instability was not observed after the same storage period. Similar results were obtained by Einhorn-Stoll, Weiss, and Kunzek (2002), who observed a rapid destabilization of emulsions prepared by a single step with Ultra-turrax. The ultrasonic bath was considered not suitable for the formation of these nanoemulsions because, after 10 min, it did not produce the emulsification of the entire oil phase.

According to these results, emulsification by high intensity ultrasonication was selected as the emulsification procedure for the next experiments. However, ultrasonication requires a large amount of energy when used directly to emulsify two separate phases; therefore, a pre-emulsification stage might be preferred to first prepare a coarse emulsion (Canselier, Delmas,

Wilhelm, & Abismaïl, 2002). In this context, the possibility of adding such a pre-emulsification step using a vortex or a high speed blender was evaluated. Table 2 shows that the smallest droplet size (111.0 ± 0.8 nm) was obtained when this pre-emulsification was performed using the high speed blender. According to all the results obtained in this section, emulsification by high intensity ultrasonication preceded by a pre-emulsification with a high speed blender (29000 rpm, 5 min) was the method selected for carrying out the experiments presented in the next sections.

3.3. Influence of oil and surfactant concentration and ultrasonication time on nanoemulsions droplet size. Search of the optimal conditions by RSM.

The results on the RSM used to optimize the formulation of wheat bran nanoemulsions with the minimum droplet size, taking into account the process variables, oil and surfactant concentration and ultrasonication time, are firstly presented. Additionally, stability of the different nanoemulsions is discussed.

3.3.1. Model fitting

The droplet size of the wheat bran nanoemulsions obtained in the experiments corresponding to the CCD design is given in Table 3. The experimental data were fitted to a quadratic polynomial equation, which was able to correctly predict the droplet size of the emulsions. The model obtained was robust, showed no lack of fit (p value was higher than 0.05, Table 4) and a high value of the correlation coefficient (R^2 = 0.986) and the distribution of the residuals was normal. All the coefficients of the quadratic polynomial model (eq. (2)) were statistically significant ($p < 0.05$) except for the interactive coefficient α_{13} (Table 4). F values indicate that, for the range of surfactant concentration studied, the oil content and ultrasonication time had stronger incidence on the droplet size of the emulsions than the

surfactant content. F values also indicate that the interaction with the highest incidence was the one occurring between the quantity of surfactant and the ultrasonication time.

3.3.2. Response surface analysis

In order to study the effect of the independent variables on the droplet size, surface response and contour plots of the quadratic polynomial model were generated by varying two of the independent variables within the experimental range while holding the third one constant at the central point. Fig. 1a was generated by varying the oil and surfactant content in the emulsion while holding constant the ultrasonication time at 175 s. It shows that, at constant oil content, an increase of surfactant content between 1 and 7% (w/w) results in a decrease of droplet size of the emulsion, while a surfactant content higher than 7% results in a droplet size increase. This could be explained by the role of the surfactant in the emulsion, since its concentration determines the total droplet surface area, the diffusion rate and the adsorption phenomena of the surfactant onto the newly formed droplets. Excessive surfactant content might lead to a lower diffusion rate of surfactants which can result in the coalescence of the emulsion droplets (Li & Chiang, 2012).

The effect of oil content and ultrasonication time on the droplet size at a fixed surfactant content of 5.5% can be observed in Fig. 1b. This Figure shows that the droplet size of the nanoemulsion increases both with ultrasonication time and oil content. Ultrasonication time is an important emulsification parameter, since it affects the adsorption rate of the surfactants to the droplet surface and the droplet size distribution (Li & Chiang, 2012). The increase of the droplet size of the emulsion when the ultrasonication time is increased has been described in the literature and it is due to the over-processing of the emulsion (Fathi, Mozafari, & Mohebbi, 2012; Kentish, Wooster, Ashokkumar, Balachandran, Mawson, & Simons, 2008; Li & Chiang, 2012). This effect makes necessary the optimization of the ultrasonic energy

309 intensity input for the system under study (Chandrapala, Oliver, Kentish, & Ashokkumar,
310 2012). The same effect of ultrasonication time and surfactant content on the droplet size of the
311 emulsions, previously discussed, was also observed when holding constant the oil content
312 (Fig. 1c).

313 *3.3.3. Stability of wheat bran oil nanoemulsions*

314 Once the influence of the process variables on the droplet size has been evaluated, it is
315 important to check if there are some important effects of these variables on emulsion stability,
316 since this is one of the most important parameters for their application.

317 Zeta potential provides information on emulsion stability and is determined by measuring the
318 velocity of charged droplets or colloids in an electrical potential field of known strength. Oil
319 droplets in an O/W emulsion exhibit a net charge at the droplet surface. It is usually a
320 negative charge, and as described by the Helmholtz theory of the electrical double layer, the
321 negative charges are aligned or closely bound to the interface. These charges attract
322 counterions from the bulk solution which give rise to a zone of opposite sign, forming an
323 electrical double layer that causes oil droplets to repel one another. Hence, zeta potential is an
324 indication of the repulsive forces between emulsion oil droplets, thus characterizes
325 coalescence/flocculation capacity of emulsions and reflects its stability (Kumar, Mishra,
326 Malik, & Satya, 2013). Large zeta potential values (positive or negative) indicate difficulty
327 for coalescence of droplets and therefore high emulsion stability. The zeta potential of the
328 emulsions corresponding to the CCD experiments varies from -30 to -40 mV, indicating good
329 stability.

330 The stability of the emulsions was also evaluated in terms of their droplet size growth and
331 appearance when they were stored during 15 and 30 days at lightness and ambient

temperature and when they were stored at 4 ºC and darkness. There was little change in the droplet size of the emulsions during storage (data not shown) but significant changes in their appearance were detected in terms of sedimentation. Sedimentation is a reversible destabilization phenomena in emulsions while modification on the droplet size is an irreversible one (Abismaïl, Canselier, Wilhelm, Delmas, & Gourdon, 1999). Visual evaluation of the emulsions formulated in this work showed that sedimentation was higher in the emulsions with higher oil content. Emulsions stored at 4 ºC and darkness showed less sedimentation than those emulsions stored at ambient temperature and lightness when their visual appearance was evaluated.

3.3.4. Optimal conditions for preparing wheat bran oil nanoemulsions

The optimal conditions for the emulsification of the WBO used in this work would be those leading to a stable emulsion with the minimum droplet size. According to the RSM results, the minimum droplet size (39.4 nm) was predicted to be achieved by combining 1.0% (w/w) WBO, 7.3% (w/w) surfactant and an ultrasonication time of 50 seconds.

It should be noted that the surfactant to oil ratio of the optimal wheat bran emulsion is relatively high what in practice is not desirable due to economic, sensorial and regulatory reasons (Qian & McClements, 2011). In any case, this is a minor problem when nanoemulsions are going to be applied as diluted forms, as in the case of this work, which objective is obtaining an emulsion with the minimum droplet size in order to improve the bioavailability of the WBO antioxidant compounds.

A confirmation of the results using the optimum conditions (1% oil, 7.3% surfactant and 50 s ultrasonication) was carried out by performing five replicates. The average droplet size obtained was of 39.9 ± 0.4 nm. The results showed that there was no significant difference (*p*

355 > 0.05) between experimental and predicted values. The low PDI obtained (0.249 ± 0.012)
356 indicates a narrow distribution of the droplet size.

357 3.4. Characterization of the optimal nanoemulsion

358 Besides determining the average droplet size and PDI of the optimal nanoemulsion some
359 other parameters were evaluated for further characterization. The zeta potential was found to
360 be -22 ± 2 mV and pH 4.9 ± 0.1. The low turbidity of the optimal nanoemulsion (600 nm
361 absorbance = 0.36 ± 0.01) is related to their small droplet size which is below the detection
362 limit of the human eye (around 50 nm) (Leong, Wooster, Kentish, & Ashokkumar, 2009).
363 This fact makes this nanoemulsion suitable for its incorporation into different systems without
364 altering their visual quality. Also, the stability during storage and the antioxidant and
365 inhibitory tyrosinase activities of WBO optimal nanoemulsion were evaluated.

366 *3.4.1. Stability along storage*

367 There was no significant change in droplet size for the optimal nanoemulsions after 15 and 60
368 days of storage at 4ºC (Fig. 2a), with no noticeable changes on visual emulsion stability.
369 However, creaming stability measurements for 60 days at 25ºC using the Turbiscan Lab
370 Expert apparatus (Fig. 2b) showed that there was a slight backscattering increase along time
371 for the middle zone of the measurement cell, which indicates an increase in droplet size
372 caused by the coalescence of oil droplets. The formation of a sedimentation front at the
373 bottom of the sample (about 3 mm of cell height) was also observed during the last days,
374 indicating a tiny emulsion destabilization at the end of the storage period.

3.4.2. Evaluation of the antioxidant activity

The antioxidant activity of the optimal nanoemulsion was evaluated by the ABTS, DPPH and FRAP methodologies. The values obtained were found to be 2729 ± 89 µmol Trolox/L emulsion, 222 ± 7 µmol Trolox/L emulsion and 471 ± 9 µmol Fe (II)/L emulsion respectively.

In order to compare the antioxidant activity of the O/W nanoemulsions with the antioxidant activity of the oil without emulsification (Rebolleda, Beltrán, Sanz, & González-Sanjosé, 2013), antioxidant activity of the nanoemulsions has been calculated by mass unit of oil in the emulsion. The FRAP values obtained for the emulsion were much lower than those obtained for the non-emulsified oil (around 49 µmol Fe (II)/g oil contained in the nanoemulsions, against 228 µmol Trolox/g oil without emulsification). However, similar results were obtained for ABTS values (around 278 µmol Trolox/g oil contained in the nanoemulsions and 270 µmol Trolox/g oil without emulsification) and DPPH values (around 23 µmol Trolox/g oil contained in the nanoemulsions and 26 µmol Trolox/g oil without emulsification). These results might be explained considering different factors, but the accessibility and affinity of the analytical reactant for the antioxidant compounds are probably the most important ones. It is also important to have in mind that the antioxidant capacity of the nanoemulsions is measured directly while the non-emulsified oil is previously dissolved in ethanol. These considerations help to understand why DPPH, which is dissolved in methanol, a solvent capable of dissolving both the non-emulsified oil and the emulsion to form a homogeneous phase, provides similar values for the emulsion and the non-emulsified oil. On the contrary, FRAP values are fairly different because both, accessibility and affinity of the analytical reactant and antioxidant compounds are fairly limited. FRAP reacts only with hydrophilic compounds, as phenols, and these compounds remain at least partially retained in the emulsion while they are totally accessible in the non-emulsified oil after being dissolved in

399 ethanol. Finally, the affinity of ABTS with both, lipophilic and hydrophilic types of
400 antioxidants, (Rivero-Pérez, Muñiz, & González-Sanjosé, 2007) explains the similar values
401 obtained for the emulsion and the non-emulsified oil in this case.

402 *3.4.3. Determination of tyrosinase inhibition activity*

403 Inhibition of food browning is one of the most constant worries of the food industry. The use
404 of natural inhibitors of polyphenol oxidases is stimulated by the need to replace the sulfite
405 agents, commonly applied as food anti-browning agents, since they are related to allergic
406 reactions. Also, cosmetic and pharmaceutical industries demand tyrosinase inhibitors to
407 prevent melanin-related health problems in humans (Maisuthisakul & Gordon, 2009).

408 The inhibitory effect of the optimal nanoemulsion on the tyrosinase activity was calculated
409 according to Equation 1. Under the assay conditions used in this work, the inhibition of the
410 mushroom tyrosinase depends on the nanoemulsion concentration, ranging from 31 to 54 %
411 for 0.5 to 2.5 % of nanoemulsion concentration. The IC_{50} for the optimal nanoemulsion was
412 estimated from the inhibition experimental data and was found to be 2.3% (v/v). This value
413 corresponds to an oil content of 222.1 µg oil/mL and to an alkylresorcinol content of 10.39 µg
414 AR/mL. Zhuang, Hu, Yang, Liu, Qiu, Zhou, et al. (2010) studied the inhibitory kinetics of
415 cardol triene (C15:3), a resorcinolic lipid isolated from cashew nut shell, on mushroom
416 tyrosinase. These authors found that cardol triene was a powerful inhibitor showing an IC_{50}
417 value of 7.1 µg/mL. It must be pointed out that no comparison for IC_{50} values can be easily
418 established since different experimental conditions have been used. Additionally, each
419 antioxidant exhibits different inhibition capacity and it is also well-known that isolated
420 substances and substances included in complex matrices, as is the case of WBO, usually do
421 not show the same antioxidant capacity. Therefore, further studies are necessary to establish
422 the mechanism and the inhibition kinetics of wheat bran oil nanoemulsions.

4. Conclusions

Wheat bran oil can be successfully incorporated into water systems by the formulation of nanoemulsions. Optimization of process conditions by RSM showed that nanoemulsions with a droplet size of 40 nm can be obtained with a combination of high speed blender (29000 rpm- 5 min) and ultrasonic processor (50 seconds) using 1% of WBO and 7.3% of a surfactant mixture (Span 80 (37.4%) and Tween 80 (62.6%)). Nanoemulsions showed good stability when stored at 4ºC during 60 days and only a small destabilization was observed in the last days of the storage when stored at 25ºC during 60 days.

Nanoemulsions prepared under the reported conditions showed relevant antioxidant properties when they were evaluated by different methods. Furthermore, results showed that nanoemulsions could have an inhibitory effect on mushroom tyrosinase activity.

5. Acknowledgments

This work is part of the GALANG project (Ref.: ITC-20113029) financed by the Spanish Government through CDTI. The authors gratefully acknowledge to the Department of Chemical and Environmental Engineering of the University of Oviedo (Spain) the opportunity of using the Turbiscan Lab Expert equipment. S.R. acknowledges the PIRTU program of the JCyL Education Ministry and the European Social Fund.

References

Abismaïl, B., Canselier, J. P., Wilhelm, A. M., Delmas, H., & Gourdon, C. (1999). Emulsification by ultrasound: drop size distribution and stability. *Ultrasonics Sonochemistry, 6*(1–2), 75-83.

444 Allende, D., Cambiella, Á., Benito, J. M., Pazos, C., & Coca, J. (2008). Destabilization-
445 enhanced centrifugation of metalworking oil-in-water emulsions: effect of
446 demulsifying agents. *Chemical Engineering & Technology, 31*(7), 1007-1014.

447 Canselier, J. P., Delmas, H., Wilhelm, A. M., & Abismaïl, B. (2002). Ultrasound
448 emulsification—an overview. *Journal of Dispersion Science and Technology, 23*(1-3),
449 333-349.

450 Chandrapala, J., Oliver, C., Kentish, S., & Ashokkumar, M. (2012). Ultrasonics in food
451 processing. *Ultrasonics Sonochemistry*, *19*(5), 975-983.

452 Chen, Q.-X., Song, K.-K., Qiu, L., Liu, X.-D., Huang, H., & Guo, H.-Y. (2005). Inhibitory
453 effects on mushroom tyrosinase by *p*-alkoxybenzoic acids. *Food Chemistry, 91*(2),
454 269-274.

455 Einhorn-Stoll, U., Weiss, M., & Kunzek, H. (2002). Influence of the emulsion components
456 and preparation method on the laboratory-scale preparation of o/w emulsions
457 containing different types of dispersed phases and/or emulsifiers. *Food / Nahrung,*
458 *46*(4), 294-301.

459 Fathi, M., Mozafari, M. R., & Mohebbi, M. (2012). Nanoencapsulation of food ingredients
460 using lipid based delivery systems. *Trends in Food Science & Technology, 23*(1), 13-
461 27.

462 Ghosh, V., Mukherjee, A., & Chandrasekaran, N. (2013). Ultrasonic emulsification of food-
463 grade nanoemulsion formulation and evaluation of its bactericidal activity. *Ultrasonics*
464 *Sonochemistry, 20*(1), 338-344.

Herrero, M., Cifuentes, A., & Ibañez, E. (2006). Sub- and supercritical fluid extraction of functional ingredients from different natural sources: Plants, food-by-products, algae and microalgae: A review. *Food Chemistry, 98*(1), 136-148.

Huang, Q., Yu, H., & Ru, Q. (2010). Bioavailability and delivery of nutraceuticals using nanotechnology. *Journal of Food Science, 75*(1), R50-R57.

Jafari, S. M., He, Y., & Bhandari, B. (2007). Production of sub-micron emulsions by ultrasound and microfluidization techniques. *Journal of Food Engineering, 82*(4), 478-488.

Karadag, A., Yang, X., Ozcelik, B., & Huang, Q. (2013). Optimization of preparation conditions for quercetin nanoemulsions using response surface methodology. *Journal of Agricultural and Food Chemistry, 61*(9), 2130-2139.

Kentish, S., Wooster, T. J., Ashokkumar, M., Balachandran, S., Mawson, R., & Simons, L. (2008). The use of ultrasonics for nanoemulsion preparation. *Innovative Food Science & Emerging Technologies, 9*(2), 170-175.

Kumar, P., Mishra, S., Malik, A., & Satya, S. (2013). Preparation and characterization of *Mentha x piperita* oil emulsion for housefly (*Musca domestica L.*) control. *Industrial Crops and Products, 44*(0), 611-617.

Leong, T. S. H., Wooster, T. J., Kentish, S. E., & Ashokkumar, M. (2009). Minimising oil droplet size using ultrasonic emulsification. *Ultrasonics Sonochemistry, 16*(6), 721-727.

485 Li, P.-H., & Chiang, B.-H. (2012). Process optimization and stability of D-limonene-in-water
486 nanoemulsions prepared by ultrasonic emulsification using response surface
487 methodology. *Ultrasonics Sonochemistry, 19*(1), 192-197.

488 Maisuthisakul, P., & Gordon, M. H. (2009). Antioxidant and tyrosinase inhibitory activity of
489 mango seed kernel by product. *Food Chemistry, 117*(2), 332-341.

490 McClements, D. J. (2005). *Food emulsions: principles, practice, and techniques* (2nd ed.).
491 Boca Ratón.

492 McClements, D. J. (2011). Edible nanoemulsions: fabrication, properties, and functional
493 performance. *Soft Matter, 7*(6), 2297-2316.

494 Peshkovsky, A. S., Peshkovsky, S. L., & Bystryak, S. (2013). Scalable high-power ultrasonic
495 technology for the production of translucent nanoemulsions. *Chemical Engineering*
496 *and Processing: Process Intensification, 69*(0), 77-82.

497 Qian, C., & McClements, D. J. (2011). Formation of nanoemulsions stabilized by model food-
498 grade emulsifiers using high-pressure homogenization: Factors affecting particle size.
499 *Food Hydrocolloids, 25*(5), 1000-1008.

500 Rebolleda, S., Beltrán, S., Sanz, M. T., & González-Sanjosé, M. L. (2013). Supercritical fluid
501 extraction of wheat bran oil: characterization and evaluation of antioxidant activity. In
502 *13th International Conference on Antioxidants*. Marrakech (Morocco).

503 Rebolleda, S., Beltrán, S., Sanz, M. T., & González-SanJosé, M. L. (2014). Supercritical fluid
504 extraction of wheat bran oil. Study of extraction yield and oil quality. *European*
505 *Journal of Lipid Science and Technology, 116,* 319–327.

506 Rebolleda, S., Beltrán, S., Sanz, M. T., González-Sanjosé, M. L., & Solaesa, Á. G. (2013).
507 Extraction of alkylresorcinols from wheat bran with supercritical CO_2. *Journal of*
508 *Food Engineering, 119*(4), 814-821.

509 Rivero-Pérez, M. D., Muñiz, P., & González-Sanjosé, M. L. (2007). Antioxidant profile of red
510 wines evaluated by total antioxidant capacity, scavenger activity, and biomarkers of
511 oxidative stress methodologies. *Journal of Agricultural and Food Chemistry, 55*,
512 5476-5483.

513 Roldán, E., Sánchez-Moreno, C., de Ancos, B., & Cano, M. P. (2008). Characterisation of
514 onion (*Allium cepa* L.) by-products as food ingredients with antioxidant and
515 antibrowning properties. *Food Chemistry, 108*(3), 907-916.

516 Tadros, T., Izquierdo, P., Esquena, J., & Solans, C. (2004). Formation and stability of nano-
517 emulsions. *Advances in Colloid and Interface Science, 108–109*(0), 303-318.

518 Wu, L.-c., Chang, L.-H., Chen, S.-H., Fan, N.-c., & Ho, J.-a. A. (2009). Antioxidant activity
519 and melanogenesis inhibitory effect of the acetonic extract of *Osmanthus fragrans*: A
520 potential natural and functional food flavor additive. *LWT - Food Science and*
521 *Technology, 42*(9), 1513-1519.

522 Yang, Y., Marshall-Breton, C., Leser, M. E., Sher, A. A., & McClements, D. J. (2012).
523 Fabrication of ultrafine edible emulsions: Comparison of high-energy and low-energy
524 homogenization methods. *Food Hydrocolloids, 29*(2), 398-406.

525 Yuan, Y., Gao, Y., Mao, L., & Zhao, J. (2008). Optimisation of conditions for the preparation
526 of β-carotene nanoemulsions using response surface methodology. *Food Chemistry,*
527 *107*(3), 1300-1306.

528 Zhuang, J.-X., Hu, Y.-H., Yang, M.-H., Liu, F.-J., Qiu, L., Zhou, X.-W., & Chen, Q.-X.
529 (2010). Irreversible competitive inhibitory kinetics of cardol triene on mushroom
530 tyrosinase. *Journal of Agricultural and Food Chemistry, 58*(24), 12993-12998.

531

532

Figure Captions

Figure 1. Response surface and contour plots of the combined effects of oil and surfactant content and ultrasonication time on the droplet size of the wheat bran nanoemulsions: (a) oil and surfactant content at an ultrasonication time of 175 s; (b) oil content and ultrasonication time at a surfactant content of 5.5%; (c) surfactant content and ultrasonication time at an oil content of 5.5%.

Figure 2. Optimal nanoemulsion prepared with 1% of WBO, 7.2% Span 80:Tween 80 (37.4:62.6) and 50 seconds of ultrasounds: (a) droplet size distribution after 0, 15 and 60 days of storage at 4 ºC and darkness, (b) backscattering profiles during 60 days of storage at 25ºC and darkness.

Table 1. Surfactants used for the emulsification of WBO, their HLB numbers and mean droplet size and polydispersity index (PDI) of the emulsions obtained

Surfactant	HLB number	Droplet size (nm)	PDI
Tween 20	16.7	200.0 ± 8.1^{d}	0.352 ± 0.016
Tween 80	15.0	109.9 ± 6.6^{b}	0.370 ± 0.009
DATEM	8.0	393.2 ± 8.0^{e}	0.485 ± 0.011
Span 80:Tween 80 (37.4:62.6)	11.0	84.6 ± 1.3^{a}	0.257 ± 0.009
Span 80:Tween 80 (75:25)	7.0	171.1 ± 3.9^{c}	0.280 ± 0.012

Values with different letters in each column are significantly different (LSD test, $p < 0.05$)

Table 2. Equipment and conditions used for the emulsification of WBO and mean droplet size and polydispersity index (PDI) of the emulsions obtained

Pre-emulsification step		Emulsification step		Droplet size (nm)	PDI
Method	Time (min)	Method	Time (min)		
None		High speed blender 25000 rpm	5.0	95.6 ± 1.6 [c]	0.234 ± 0.008 [c]
None		High speed blender 29000 rpm	5.0	77.0 ± 1.1 [b]	0.225 ± 0.013 [c]
None		High speed blender 35000 rpm	5.0	66.3 ± 0.9 [a]	0.187 ± 0.005 [b]
None		Ultrasonic bath	10	-	-
None		High intensity ultrasonic processor	2.5	136.4 ± 1.3 [e]	0.121 ± 0.010 [a]
Vortex	1	High intensity ultrasonic processor	2.5	133.5 ± 1.3 [e]	0.139 ± 0.009 [a]
High speed blender 29000 rpm	5	High intensity ultrasonic processor	2.5	111.0 ± 0.8 [d]	0.132 ± 0.008 [a]

Values with different letters in each column are significantly different (LSD test, $p < 0.05$)

Table 3. Matrix of the central composite design (CCD) and experimental data obtained for the response variable (Y)

Run	Independent variables			Response variable
	WBO concentration (X_1, % w/w)	Surfactant concentration (X_2, % w/w)	Ultrasonication time (X_3, s)	Droplet size (Y, nm) (mean ± SD)
1	5.5	5.5	175	155.7 ± 9.1
2	1.0	1.0	50	81.5 ± 4.2
3	10.0	1.0	50	199.0 ± 0.7
4	1.0	10.0	50	50.7 ± 2.0
5	10.0	10.0	50	138.1 ± 0.8
6	1.0	1.0	300	116.8 ± 6.2
7	10.0	1.0	300	226.1 ± 1.3
8	1.0	10.0	300	143.6 ± 1.8
9	5.5	5.5	175	154.3 ± 4.2
10	10.0	10.0	300	247.3 ± 20.4
11	1.0	5.5	175	92.1 ± 3.4
12	10.0	5.5	175	210.4 ± 15.4
13	5.5	1.0	175	184.8 ± 2.1
14	5.5	10.0	175	174.8 ± 1.2
15	5.5	5.5	50	105.2 ± 1.3
16	5.5	5.5	300	167.4 ± 0.4
17	5.5	5.5	175	149.5 ± 1.3

Table 4. Analyses of variance of the regression coefficients of the quadratic equation (2) for the droplet size of WBO nanoemulsions

Polynomial coefficient (PC)[a]	PC-value	*F*-value	*p*-value
α_0	58.9453		
α_1	16.1043	2384.05	0.0000
α_2	-17.6021	24.05	0.0080
α_3	0.552472	884.93	0.0000
α_{11}	-0.299374	8.17	0.0460
α_{22}	1.10803	111.87	0.0005
α_{33}	-0.00134799	98.58	0.0006
α_{12}	-0.220679	13.25	0.0220
α_{13}	0.00181111	0.69	0.4533
α_{23}	0.0310333	202.18	0.0001
Lack of fit		2.55	0.1883

[a] α_0 is a constant, α_i, α_{ii} and α_{ij} are the linear, quadratic and interactive coefficients of the quadratic polynomial equation, respectively

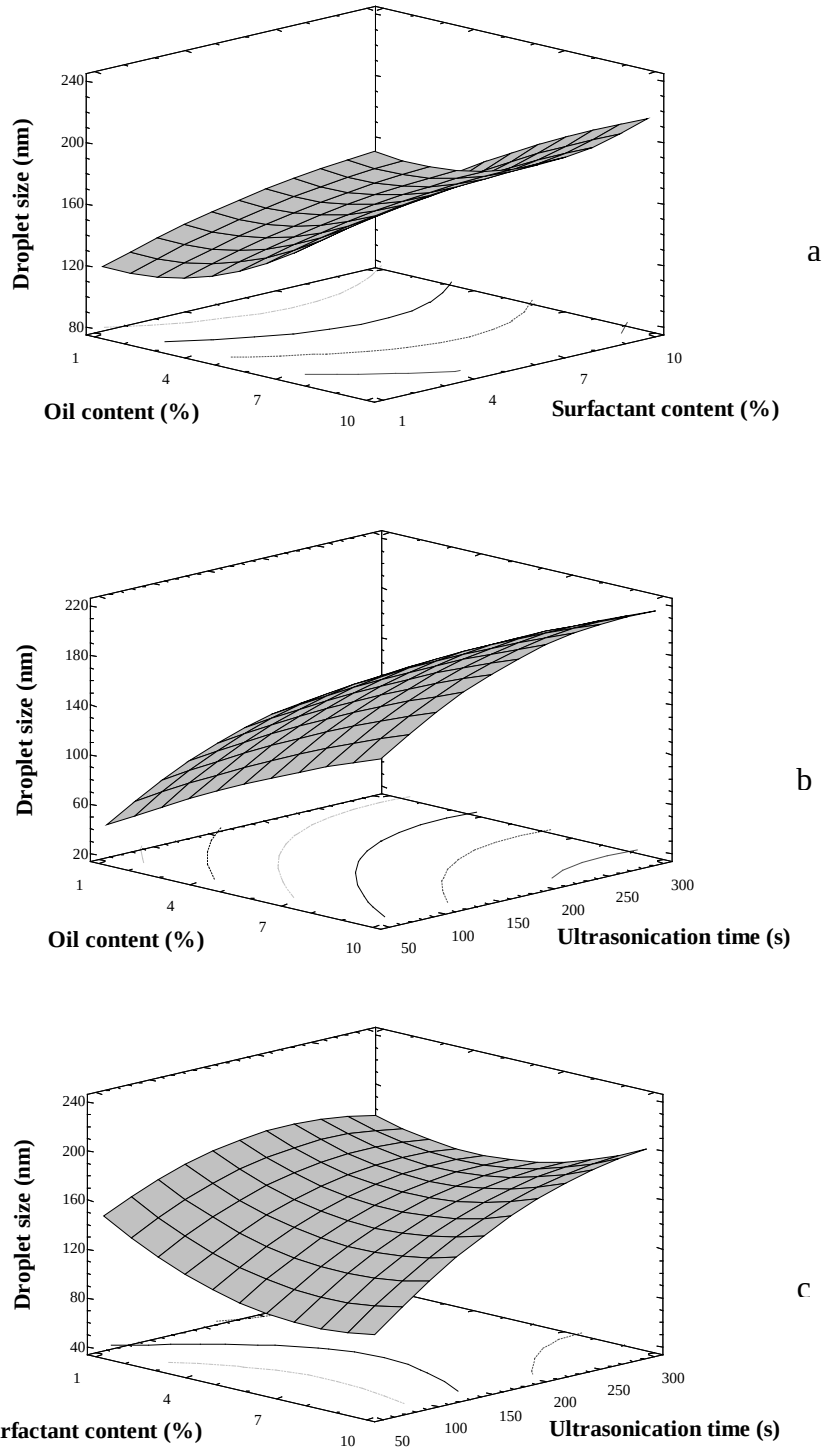

Figure 1. Response surface and contour plots of the combined effects of oil and surfactant content and ultrasonication time on the droplet size of the wheat bran nanoemulsions: (a) oil and surfactant content at an ultrasonication time of 175 s; (b) oil content and ultrasonication time at a surfactant content of 5.5%; (c) surfactant content and ultrasonication time at an oil content of 5.5%.

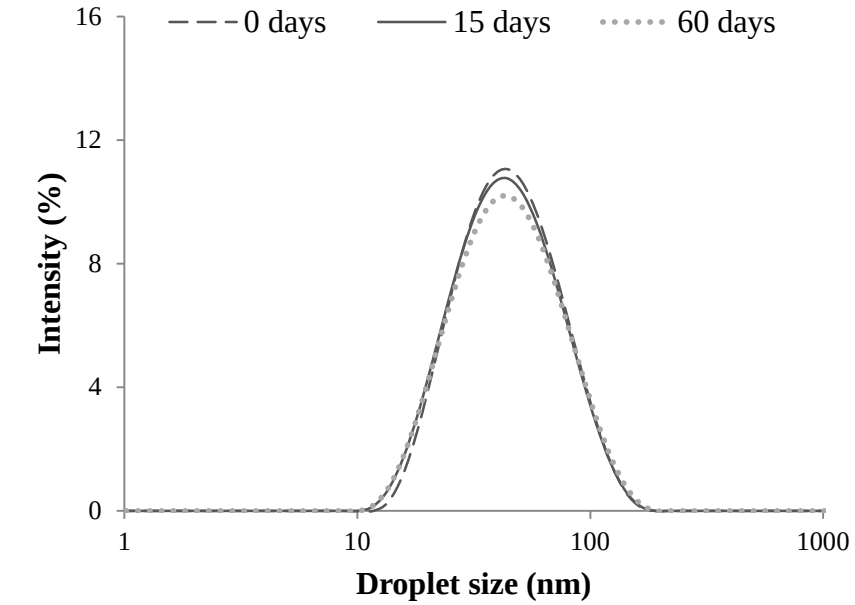

a

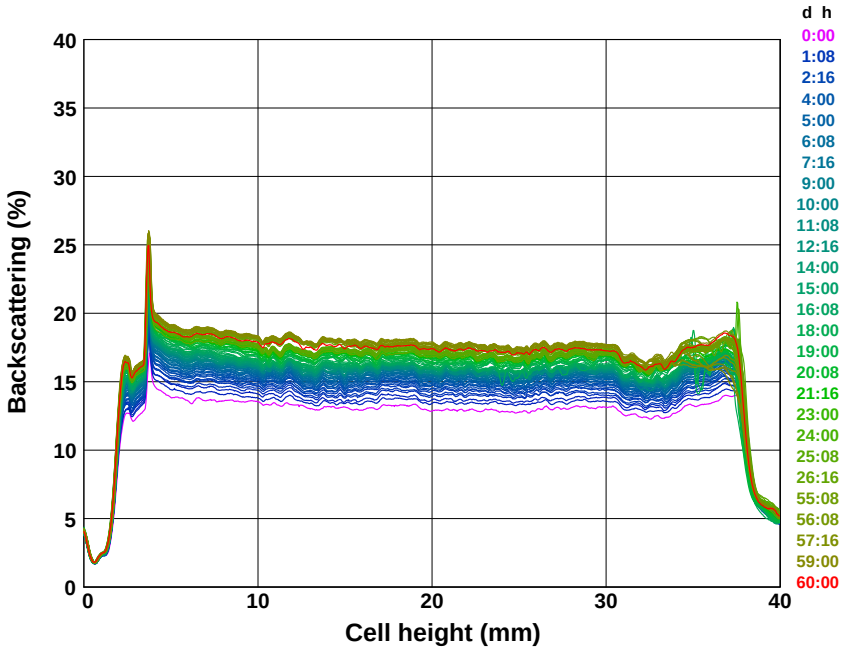

b

Figure 2. Optimal nanoemulsion prepared with 1% of WBO, 7.3% Span 80:Tween 80 (37.4:62.6) and 50 seconds of ultrasounds: (a) droplet size distribution after 0, 15 and 60 days of storage at 4 ºC and darkness, (b) backscattering profiles during 60 days of storage at 25ºC and darkness.